Journal of Sound and Vibration (1998) **214**(4), 747–759
Article No. sv981607

DYNAMIC ANALYSIS OF RIGID SURFACE FOOTINGS BY BOUNDARY ELEMENT METHOD

J. QIAN
Institute of Engineering Structures, Tongji University, Shanghai, P.R. China

AND

L. G. THAM AND Y. K. CHEUNG
Department of Civil and Structural Engineering, University of Hong Kong, Hong Kong

(*Received* 23 *October* 1997, *and in final form* 2 *March* 1998)

An accurate and efficient boundary element procedure is developed for the analysis of dynamic response of rigid surface footings. The footings are assumed to be resting on an elastic half-space. The problem is formulated in the frequency domain by adopting the half-space Green's function for surface points loads. Therefore, only discretization is required for the soil–footing interface. Two types of element, linear and quadratic isoparametric elements, are employed for the discretization. Examples of the single-footing as well as two-footing system are presented to demonstrate the application of the method. The results are compared with other published results. It is demonstrated that the present results are in good agreement with the approximate solution proposed by Tajimi at low frequency range. However, the approximate solution may lead to an over-estimation of the amplitude and decaying rate as the frequency increases.

1. INTRODUCTION

The dynamic interaction of footings resting on the surface of a soil medium has been one of the main interests of research over the years. In the case of a group of footings, not only the interaction between each footing and the soil but also the interaction through the soil between adjacent footings has to be considered. Various solutions were proposed to solve this problem. For a footing system consisting of a small number of footings having regular shapes, such as circular, square and rectangular, semi-analytic solutions proposed by Triantafyllidis and Prange [1, 2] and Liou [3] provided highly accurate results. However, the complexity of geometries and boundary conditions involved in engineering practice have greatly limited the applications of such analytical procedures. Therefore, numerical methods, such as the finite element method (FEM) and the boundary element method (BEM), were developed to investigate the dynamic interaction or cross-interaction problem [4–6]. It is well known that the BEM has its distinct advantages over FEM in studying this problem [6]. Most of BEM solutions used constant elements because of its simplicity. However, extensive numerical studies [7] reveal that, in some cases, use of constant elements causes certain numerical problems in computation.

On the other hand, some simplified approaches for computing the dynamic response of rigid surface footings were proposed by Kitamura and Sakurai [8] and Chow [9]. They were based on almost the same line as conventional BEM by discretizing the contact area into subregions and no numerical integration was required to evaluate the influence coefficients. An approximate expression further derived by Tajimi [10] was adopted to compute the

0022–460X/98/290747 + 13 $30.00/0

influence outside the loaded subregion so that large amounts of computation can be saved. This improves the efficiency in the analysis of the interaction of group of footings. Unfortunately, significant errors may arise from the substitution of Tajimi's point-to-point approximation for two finite subregions.

In this paper, a detailed numerical investigation is carried out on the dynamic interaction of a group of footings using the boundary element procedure developed by the author [4, 11]. The proposed BEM scheme is based on the frequency domain half-space Green's function and is found to be effective for two closely placed footings up to a vanishing small separation. In the analysis, both linear and quadratic discretizations are employed. Validation of the Tajimi's approximation for computing the coupling influence coefficients is also discussed.

2. BEM FORMULATION FOR DYNAMIC INTERACTION ANALYSIS

The response of a rigid surface footing resting on a uniform elastic half-space under the action of harmonic excitations, either external forces or incident seismic waves, is considered. The motion of such a system can be described in terms of the six generalized displacement components as shown in Figure 1.

$$\{\Delta\} = [\Delta_1, \Delta_2, \Delta_3, \Phi_1, \Phi_2, \Phi_3]^{\mathrm{T}} \tag{1}$$

where Δ_i and $\Phi_i (i = 1, 2, 3)$ are the rigid body displacements and rotations, respectively, at the centre of the footing. The compatibility of displacements at the contact region requires that

$$\{U\} = [S]\{\Delta\} \tag{2}$$

where $\{U\}$ is the displacement vector on the surface of the half-space and $[S]$ is the transform matrix. The submatrix of $[S]$ for each node can be written as

$$[S]^{\mathrm{sub}} = \begin{bmatrix} 1 & 0 & 0 & 0 & 0 & -y \\ 0 & 1 & 0 & 0 & 0 & x \\ 0 & 0 & 1 & y & -x & 0 \end{bmatrix}. \tag{3}$$

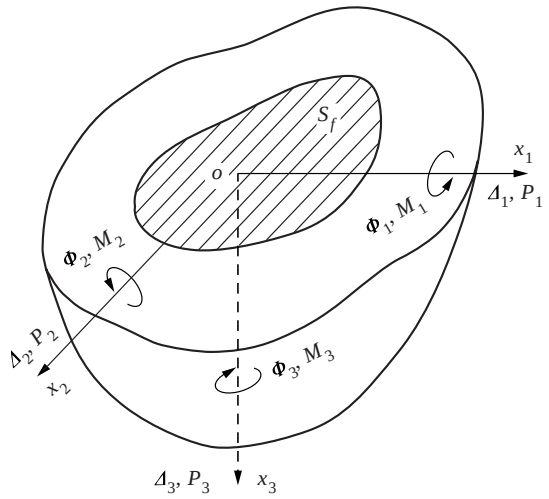

Figure 1. Geometry and coordinate system.

It can be shown readily that the resultant forces with components P_i and the resultant moments with components $M_i (i = 1, 2, 3)$ acting on the contact area can be computed from surface traction $\{t\}$ by

$$\{P\} = \int_S [S]^{\mathrm{T}}\{t\}\, \mathrm{d}S. \tag{4}$$

Due to the linearity of the problem, the displacements caused by any stress distribution on the soil–footing contact region can be calculated by using the principle of superposition. If the corresponding Green's functions are known, the relation between the displacements and tractions are:

$$\{u\} = \int_S [\bar{G}(x_1 - \xi_1, x_2 - \xi_2)]\{t\}\, \mathrm{d}\xi_1\, \mathrm{d}\xi_2. \tag{5}$$

In the above equation, $\bar{G}_{ij}(x_1 - \xi_1, x_2 - \xi_2)$ is the Green's function for the surface displacement at (x_1, x_2) in the x_i-direction due to a unit force acting at (ξ_1, ξ_2) in the x_j-direction. It can be determined directly by using double Fourier transformation and has the form [11]

$$\bar{G}_{11} = \frac{1}{2\pi\mu R}\int_0^{+\infty}\left[\frac{\kappa_s^2 R^2 (z^2 - \kappa_s^2 R^2)^{1/2}}{F(z, \kappa_s)}\cos^2\phi - \frac{\sin^2\phi}{(z^2 - \kappa_s^2 R^2)^{1/2}}\right] z J_0(z)\, \mathrm{d}z$$

$$- \frac{\cos 2\phi}{2\pi\mu R}\int_0^{+\infty}\left[\frac{\kappa_s^2 R^2 (z^2 - \kappa_s^2 R^2)^{1/2}}{F(z, \kappa_s)} + \frac{1}{(z^2 - \kappa_s^2 R^2)^{1/2}}\right] J_1(z)\, \mathrm{d}z$$

$$\bar{G}_{21} = \bar{G}_{12} = \frac{\sin 2\phi}{2\pi\mu R}\int_0^{+\infty}\left[\frac{\kappa_s^2 R^2 (z^2 - \kappa_s^2 R^2)^{1/2}}{F(z, \kappa_s)} + \frac{1}{(z^2 - \kappa_s^2 R^2)^{1/2}}\right]\left[\frac{z}{2} J_0(z) - J_1(z)\right] \mathrm{d}z$$

$$\bar{G}_{31} = -\bar{G}_{13} = -\frac{\cos\phi}{2\pi\mu R}\left\{\frac{1}{2} + \int_0^{+\infty}\frac{\kappa_s^2 R^2 (z^2 - \kappa_s^2 R^2/2)}{F(z, \kappa_s)} J_1(z)\, \mathrm{d}z\right\}$$

$$\bar{G}_{22} = \frac{1}{2\pi\mu R}\int_0^{+\infty}\left[\frac{\kappa_s^2 R^2 (z^2 - \kappa_s^2 R^2)^{1/2}}{F(z, \kappa_s)}\sin^2\phi - \frac{\cos^2\phi}{(z^2 - \kappa_s^2 R^2)^{1/2}}\right] z J_0(z)\, \mathrm{d}z$$

$$+ \frac{\cos 2\phi}{2\pi\mu R}\int_0^{+\infty}\left[\frac{\kappa_s^2 R^2 (z^2 - \kappa_s^2 R^2)^{1/2}}{F(z, \kappa_s)} + \frac{1}{(z^2 - \kappa_s^2 R^2)^{1/2}}\right] J_1(z)\, \mathrm{d}z$$

$$\bar{G}_{32} = -\bar{G}_{23} = -\frac{\sin\phi}{2\pi\mu R}\left\{\frac{1}{2} + \int_0^{+\infty}\frac{\kappa_s^2 R^2 (z^2 - \kappa_s^2 R^2/2)}{F(z, \kappa_s)} J_1(z)\, \mathrm{d}z\right\}$$

$$\bar{G}_{33} = \frac{1}{2\pi\mu R}\int_0^{+\infty}\frac{\kappa_s^2 R^2 (z^2 - n^2\kappa_s^2 R^2)^{1/2}}{F(z, \kappa_s)} z J_0(z)\, \mathrm{d}z \tag{6}$$

where μ is the shear modulus, $J_0(z)$ and $J_1(z)$ are the Bessel functions of the first kind and order 0 and 1, respectively. $k_s = \omega/c_2$, $n = c_2/c_1$, in which ω is the circular frequency, c_1

and c_2 are the dilatational and shear wave velocities respectively. $F(z, k_s)$ is the Rayleigh function,

$$F(z, k_s) = (2z^2 - k_s^2 R^2) - 4z^2(z^2 - k_s^2 R^2)^{1/2}(z^2 - n^2 k_s^2 R^2)^{1/2} \tag{7}$$

R is the distance between the source and receiver points and ϕ is its angle to the axis parallel to the x_1 axis.

One can easily prove that the influence functions of Wong and Luco [12] obtained under the assumption of uniform distribution of contact stresses are exactly the same as equation (6) when the contact area approaches zero and the contact forces are constant. However, the Green's function $[\bar{G}]$ of (6) permits the use of higher order elements so that higher order interpolations are allowed. This is an improvement over those adopted in Reference [12] which can be used for constant elements only.

3. NUMERICAL EVALUATION OF THE INTEGRAL EQUATIONS

To compute the integral equation (5), one has to discretize the contact region into a number of elements and interpolate the field variables within the element. Choosing flat boundary elements, the mathematics and programming can be very much simplified as the field variables will only have to be collocated at the centroids of each element. This implies that the contact stresses within the element are constant. The drawback of such an approach is that it is not very accurate and convergence of the results is slow [5]. In this study, the isoparametric representation of the geometry and the field variables has been used. To improve the results, linear and quadratic elements are employed in the study.

Adopting the isoparametric mapping concept, the co-ordinates and the field variables of any point within an element can be expressed in terms of the corresponding nodal values as

$$\{q\} = [N]\{Q\} \tag{8}$$

where $\{q\}$ represents the quantity within the element and $\{Q\}$ its value at the nodal points.

Due to the discretizing, equation (5) can be expressed in the discrete form as

$$\{U\} = [G]\{T\} \tag{9}$$

where $\{U\}$ and $\{T\}$ are the global vector of displacement and traction, respectively, and $[G]$ is assembled from the element matrices $[G]^e$ of the form,

$$[G]^e = \int_{s_f^e} [\bar{G}][N]|J| \, d\eta_1 \, d\eta_2 \tag{10}$$

$[N]$ is the matrix of shape functions and $|J|$ the Jacobian matrix relating the transformation from the cartesian to the local coordinate system.

In the case of rigid footings, the global rigid-body displacement vector $\{\Delta\}$ is assembled from that of equation (1) for each isolated footing. The resultant forces $\{P\}$ can also be calculated over each footing separately and the force–displacement relation for a N footings system can be written as:

$$\{P\} = [K(\omega)]\{\Delta\} \tag{11}$$

where $[K(\omega)]$ is the $6N \times 6N$ impedance or dynamic stiffness matrix of the system including cross-interaction effects between adjacent footings.

Since analytical integration of the integrals of equation (10) is impossible in most cases, a numerical quadrature technique has to be used. The integrals are non-singular if the field

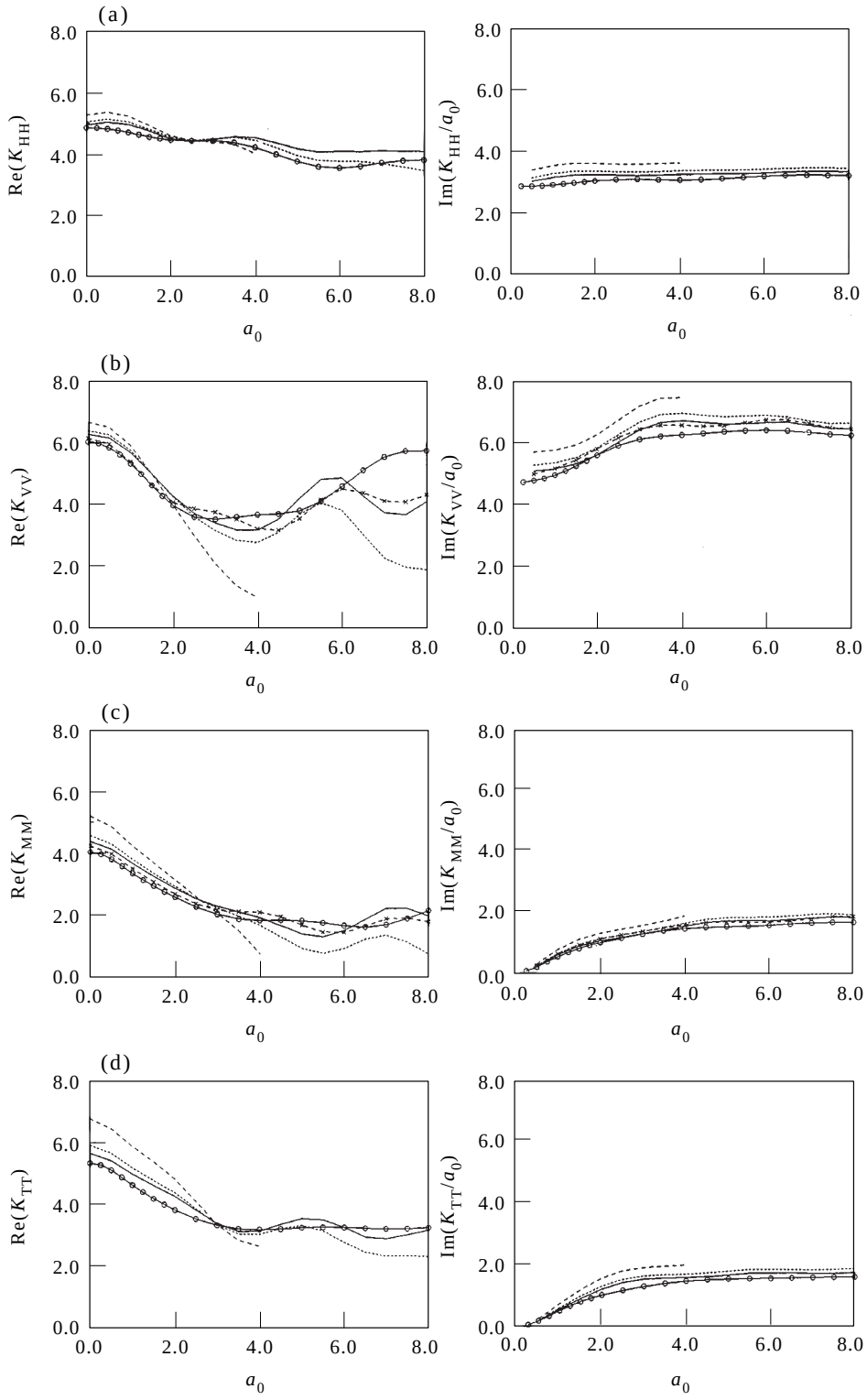

Figure 2—(*Caption on following page*).

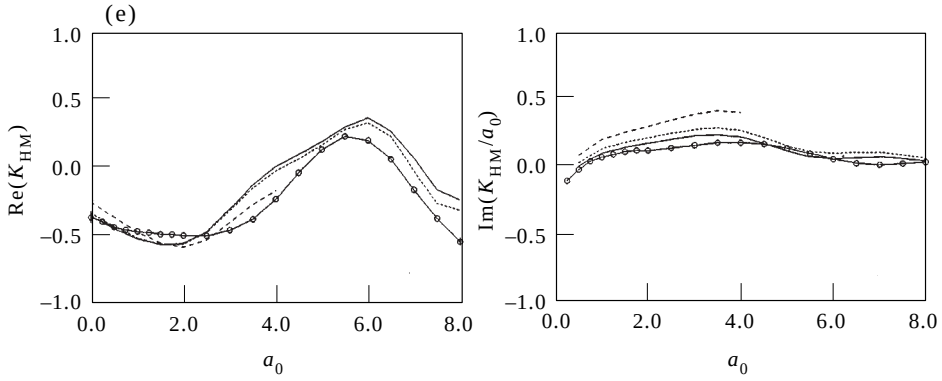

Figure 2. (a) Horizontal impedance K_{HH} of a circular foundation. (b) Vertical impedance K_{VV} of a circular foundation. (c) Rocking impedance K_{MM} of a circular foundation. (d) Torsional impedance K_{TT} of circular foundation. (e) Coupling impedance K_{HM} between horizontal and rocking. Key: —, 56 elements; - - - , 12 elements; – – –, 4 elements; ○–○, Luco and Mita [14]; * - - - *, E. R. B.

point p is outside the element. The Gauss–Legendre formula [13] is adopted for computing the integrals of the kernel-shape function products. For the singular case, it is fortunate that the integrals only contain weak singularity. Therefore, they can be accurately integrated by the sub-cell geometrical transformation technique [5]. This technique eliminates the singularity and transforms the integrand into a well-behaved function, because the behaviour of the determinant of the Jacobian matrix is approximately $O(R)$ and when combined with the kernel-shape function products ensures that the integrand of equation (10) is a bounded function throughout the region of integration.

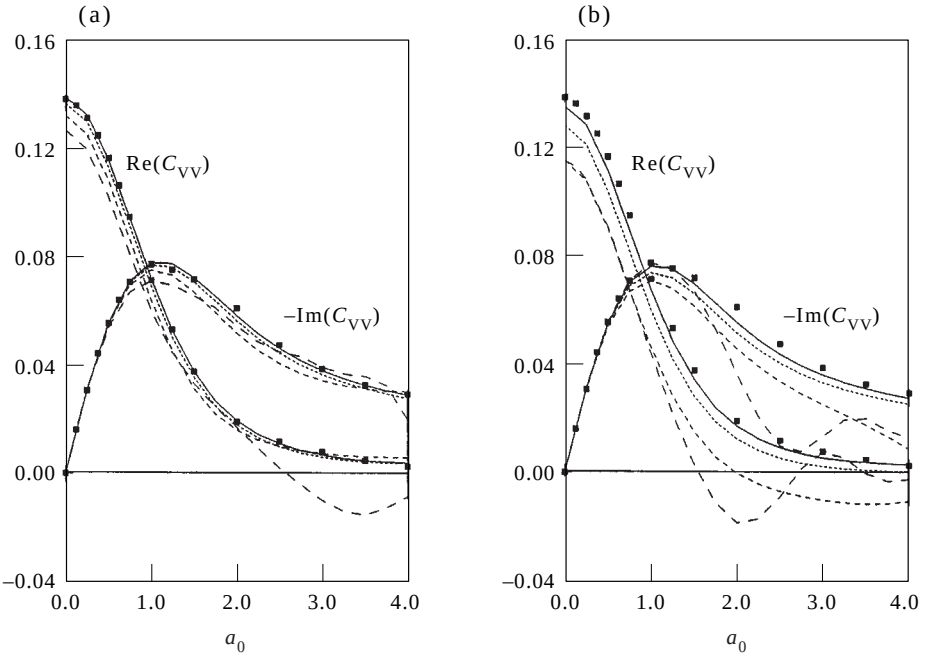

Figure 3. Convergence test (a) quadratic element, (b) linear element. Key: —, 8×8; - - - , 4 × 4; – – –, 2 × 2; — —, 1 × 1; ■, Rizzo *et al*. [15].

Due to the singular nature of Green's functions, special treatments are also required for the evaluation of equation (6). The integrands of equation (6) may have singularities at branch points and the Rayleigh pole of the Rayleigh function. For numerical purposes, the range of integration is divided into several parts in accordance with the singular points. Each of the component integrals is taken along the real axis with the exception at the Rayleigh pole for which the path is a small indentation above the pole. The last one has an infinite range $(\lambda, +\infty)$ in which λ is a large positive number. By expanding the integrand in inverse powers of z and substituting $z = 1/t$, the transformed integrals become a finite one and can be evaluated term by term by the numerical quadrature procedure.

Some difficulties may still exist since the integrands in equation (6) are highly oscillatory in certain intervals and undergo rapid variations in their values near certain values of z. The degree of irregularity increases with frequency. To deal with the irregular oscillation in the integrand, the use of a variable interval and adaptive Gaussian quadrature scheme was made in this study. This adaptive scheme automatically concentrates abscissas around regions of sharp variation in integrands, takes full advantage of efficiency of Gaussian quadrature schemes and at the same time adjusts the interval of integration as required by the complexity of the intergrand. Details of the numerical implementation can be found in Qian and Beskos [4, 11].

4. NUMERICAL STUDIES AND COMPARISONS

The results obtained by the proposed method are checked against benchmark examples. A rigid circular footing of radius a resting on an elastic half space is taken as the first example. The impedance functions of such footing are shown in Figure 2. In the figures, K_{HH}, K_{VV}, K_{MM} and K_{TT} represent the horizontal, vertical, rocking and torsional impedance, respectively. In addition, Figure 2(e) shows the result of K_{HM}, the coupling between horizontal and rocking component. The dimensionless frequency is defined as $a_0 = \omega a/c_s$. Poisson's ratio is $\nu = 1/3$. Numerical results are obtained by using 4, 12 and 56 quadratic elements. Such elements are chosen because they can approximate the curve boundary more closely. The corresponding results of Luco and Mita [14] are also shown in Figure 2. It must be pointed out that the results of reference [14] were obtained by assuming relaxed boundary conditions: the horizontal displacements are left unconstrained for vertical and rocking vibration while the vertical displacements are left unconstrained for

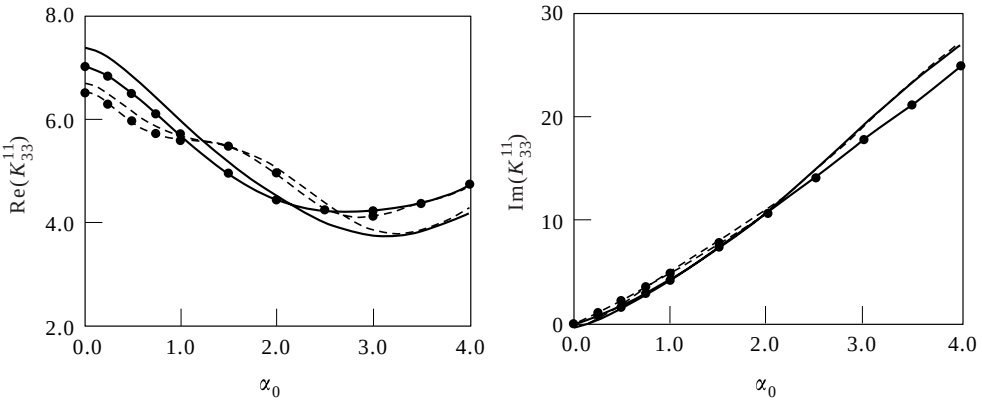

Figure 4. Vertical impedance K_{33}^{11} for the two-circular footing system. $d/a = 0{\cdot}2$, ——, present BEM, ●—● Liou [3]; $d/a = 1{\cdot}0$, - - - , present BEM, ● - - ●, Liou [3].

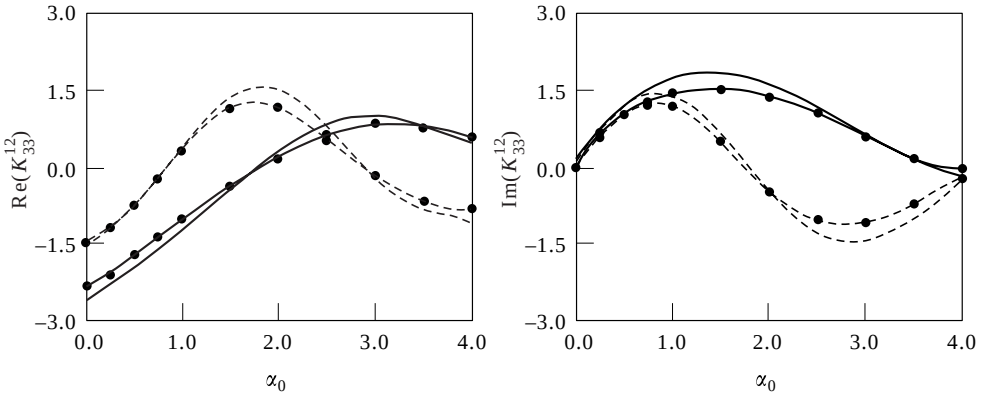

Figure 5. Coupling vertical impedance K_{33}^{12} between two circular footings. $d/a = 0{\cdot}2$, ——, present BEM, ●—● Liou [3]; $d/a = 1{\cdot}0$, - - -, present BEM, ● - - ●, Liou [3].

horizontal vibrations. Compared with the results of Luco and Mita [14], the agreement is excellent, especially when the same relaxed boundary (R.B.) condition is also adopted in the present study. It is also noted that impedance functions at high frequencies cannot be reasonably calculated by using a small number of elements, and therefore, comparison is made for low frequencies only for the results of coarse mesh (4 elements).

Numerical convergence test has been made for both linear and quadratic elements. The vertical compliance function C_{VV} for a rigid square footing of sides $2a$ is evaluated. Figure 3

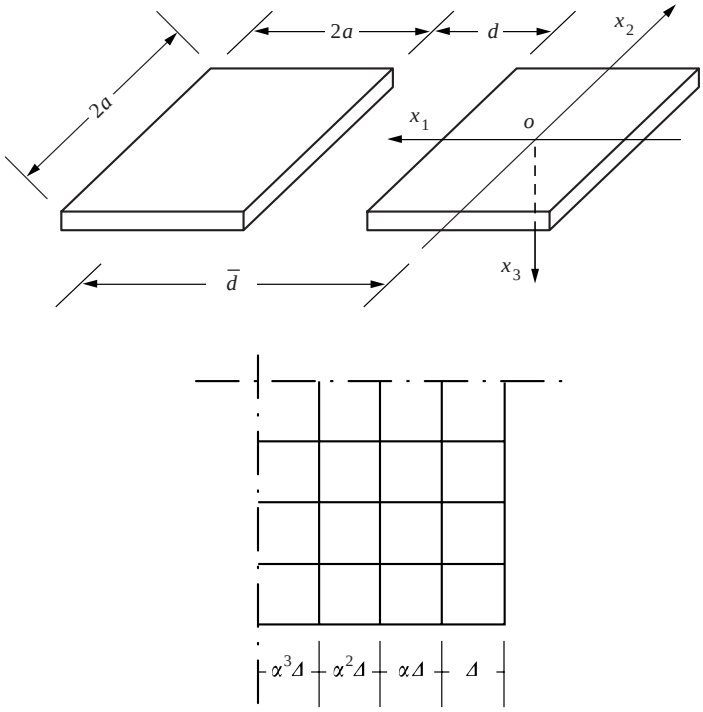

Figure 6. Two-footing model and discretization.

shows that, as the total number of elements increases, the results of both linear and quadratic elements converge. Of course, the quadratic element converges more rapidly and is preferable for use in future studies. Compared with the results of Rizzo *et al*. [15], which were obtained by using the full-space Green's function in conjunction with quadratic elements, the agreement is again excellent.

For a two-footing system, the force–displacement relationship of equation (11) can be rewritten in submatrices form as

$$\begin{Bmatrix} \{P\}^1 \\ \{P\}^2 \end{Bmatrix} = \begin{bmatrix} [K]^{11} & [K]^{12} \\ [K]^{21} & [K]^{22} \end{bmatrix} \begin{Bmatrix} \{\Delta\}^1 \\ \{\Delta\}^2 \end{Bmatrix} \tag{12}$$

where superscripts 1 and 2 denote the quantities for footing 1 and 2, respectively. $[K]^{ij}(i, j = 1, 2)$ are 6×6 submatrices with $[K]^{12} = ([K]^{21})^{\mathrm{T}}$ representing the coupling between the footings, i.e., the induced contact forces on footing i due to the displacements of footing j. Figures 4 and 5 show the impedance functions K_{33}^{11} and K_{33}^{12} for the vertical vibration of two circular footings. Poisson's ratio of the soil is $\nu = 1/3$ and the separation between the two footings is selected to be $d/a = 0{\cdot}2$ and $1{\cdot}0$, where d is the separation distance and a the radius of the footings. It can be seen that, for both cases, the present results are in very good agreement with those of Liou [3]. It should be noted that, to avoid the singularity at the Rayleigh poles, a small amount of material damping has been assumed in the soil medium by Liou [3].

In studying cross-interaction effects between two closely spaced footings, Wong and Luco [7] found that impedance functions calculated by the BEM procedure based on the assumption of constant contact stresses may be markedly affected by surface discretization. As the separation of the two footings approaches zero, the impedance functions given by Wong and Luco [7] appear to increase without bound while those of Yoshida *et al*. [16] showed finite values. Detailed numerical comparisons are presented below for easier comprehension.

To consider the static impedance functions of a two-footing system, each footing is discretized into 8×8 surface elements by two perpendicular grids as shown in Figure 6 with $\alpha \geqslant 1{\cdot}0$. The smaller elements are located along edges where stress concentration occurs. The size of the smallest elements is given by $\Delta = a(\alpha - 1)/(\alpha^4 - 1)$. Figures 7(a) and (b) show the static horizontal impedance functions K_{11}^{11} and K_{11}^{12} vs Δ for different values of dimensionless separation d/a. It is interesting to note that the values of K_{11}^{11} and K_{11}^{12} either by Wong and Luco [7] or by the present method are approximately linear with Δ for finite values of separation d. Different trend appears only as d and Δ approach zero simultaneously. However, the sum $(K_{11}^{11} + K_{11}^{12})$ always has a bound value as shown in Figure 7(c). For $d = 0$, the term $2(k_{11}^{11} + K_{11}^{12})$ represents the horizontal impedance function for a rigid rectangular footing of dimension $4a \times 2a$. There seems to be no strong evidence that impedance functions should tend to infinity since it is believed that the coupling effects betwen two footings will not cause an even higher order of singularity than in the case of a single footing.

In view of the large amount of computer time required for evaluation of influence function G_{ij}, a simplified approximate formula for equation (6) was proposed by Tajimi [10]. This approximate formula was employed by Kitamura and Sakurai [8] and Chow [9] to study the dynamic response of rigid surface footings of arbitrary geometry. To apply Tajimi's approximation, one has assumed that the contact stresses are uniformly distributed over each discretized subregion and equivalent to the concentrated forces acting on its centre.

For instance, the Tajimi's approximation for vertical response Δ_3 at the point i due to a vertical force P_3 at the point j is given by

$$\Delta_3^i = C_{33}^{ij} \cdot P_3^i$$

$$C_{33}^{ij} = \frac{(1-\nu)}{2\pi\mu R}\, e^{-ik_1 r}, \qquad k_1 = 1{\cdot}2\omega/c_s \tag{13}$$

where R is the distance between points i and j. To evaluate the coupling influence coefficients of two discretized subregions by using equation (13) implies that the central

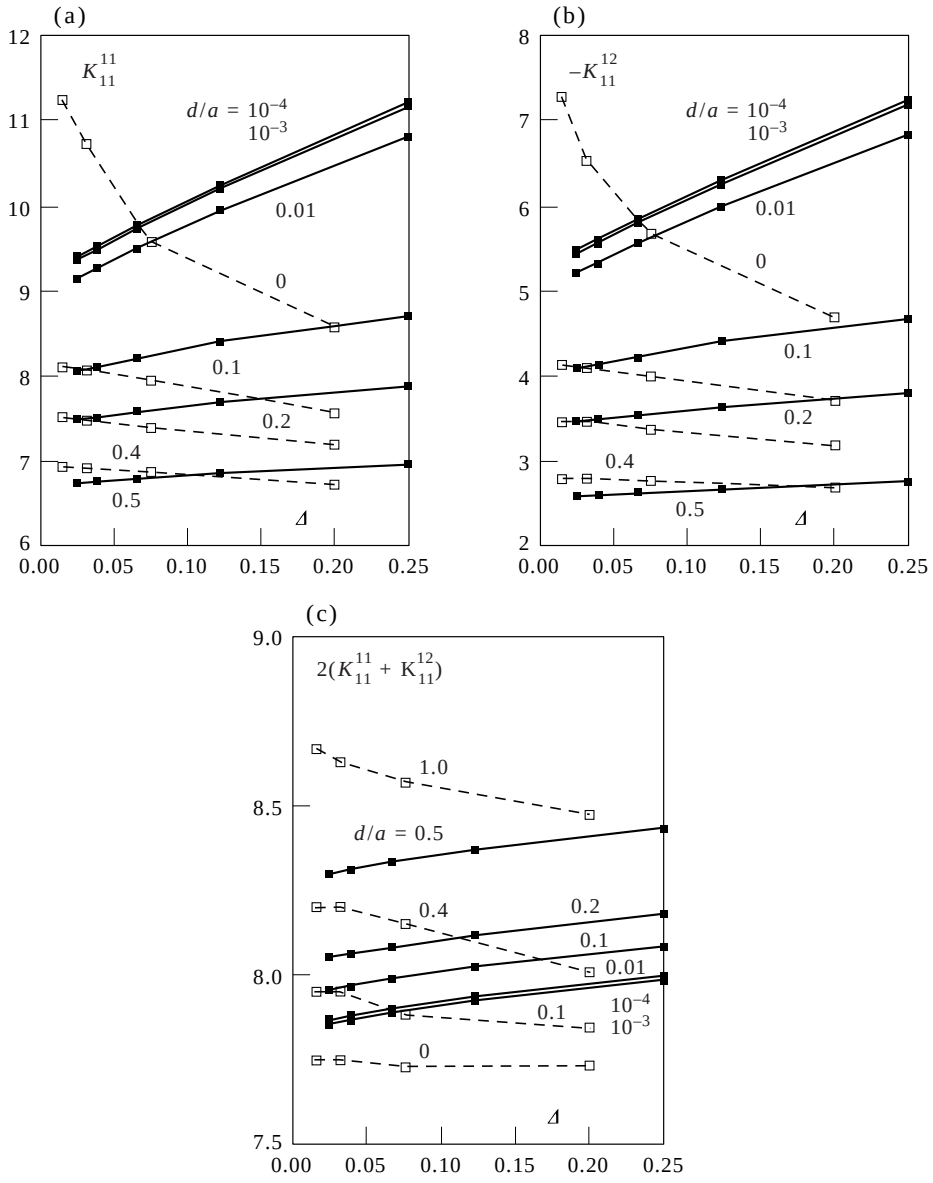

Figure 7. Effect of discretization on the static impedance functions, □ Wong and Luco [7]; ■ present BEM.

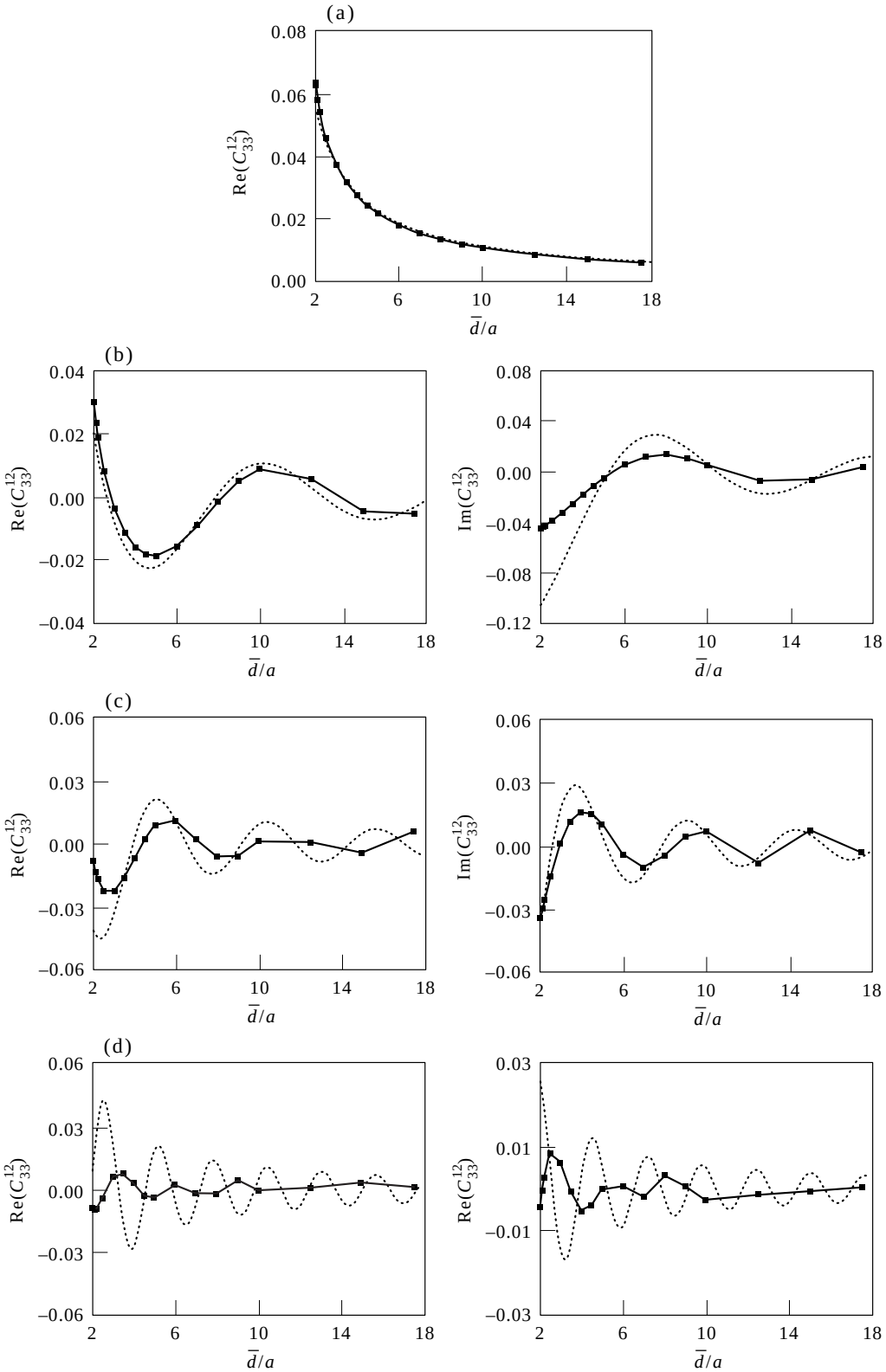

Figure 8. Vertical influence coefficient for two square subregions (a) $a_0 = 0{\cdot}0$; (b) $a_0 = 0{\cdot}5$; (c) $a_0 = 1{\cdot}0$; and (d) $a_0 = 2{\cdot}0$. Key: ■–■, BEM; - - - - -, Tajimi [10].

points of two subregions are located at i and j, respectively and their dimensions are ignored.

On the other hand, a more exact computation of the influence coefficients can be done by adopting the present method. The coupling influence coefficients can be accurately calculated by treating the two subregions as independent individuals and $[C]$ equals to the inverse of their impedance matrix $[K]$, i.e.,

$$\{\Delta\} = [C]\{P\} = [K]^{-1}\{P\}. \tag{14}$$

A comparison of results obtained by equations (13) and (14) is given in Figure 8. It appears that the approximate formula is in good agreement with present results for low frequencies only. As the frequency increases, there are considerable differences between the two sets of results. Similar conclusions can be drawn for the horizontal components of the response.

5. CONCLUSIONS

An accurate and efficient boundary element methodology for the dynamic analysis of 3-D rigid surface footings subjected to harmonic external force excitation has been developed and fully tested. High order isoparametric elements are used in this study. Compared with the constant elements, the present procedure has the advantage of yielding higher accuracy and achieving rapid convergence, as well as the possibility for it to accommodate complicated geometry. Numerical studies reveal that the use of Tajimi's approximation to evaluate the coupling influence coefficients may lead to unexpected inaccuracy for dynamic cases.

ACKNOWLEDGMENTS

The first author appreciates the award of a Research Grant of the National Education Commission of China and a Tongji University Research Grant for preparing part of this paper. The support of the Croucher Foundation is also acknowledged.

REFERENCES

1. Th. Triantafyllidis and B. Prange 1987 *Soil Dynamics & Earthquake Engineering* **6**, 164–179. Dynamic subsoil-coupling between rigid rectangular foundations.
2. Th. Triantafyllidis and B. Prange 1989 *Soil Dynamics & Earthquake Engineering* **8**, 9–21. Dynamic subsoil-coupling between rigid circular foundations on the half-space.
3. G. S. Liou 1994 *Earthquake Engineering & Structural Dynamics* **23**, 193–210. Dynamic stiffness matrices for two circular foundations.
4. J. Qian and D. E. Beskos 1995 *Earthquake Engineering & Structural Dynamics* **24**, 419–437. Dynamic interaction between 3-D rigid surface foundations and comparison with the ATC-3 provisions.
5. G. B. Manolis and D. E. Beskos 1988 *Boundary Element Methods in Elastodynamics*. London: Unwin Hyman.
6. D. E. Beskos 1993 in *Developments in Dynamic Soil-Structure Interaction*, (P. Gulkan and R. W. Clough, editors) 61–90. Dordrecht: Kluwer Academic. Application of the boundary element method in dynamic soil-structure interaction.
7. H. L. Wong and J. E. Luco 1986 *Soil Dynamics & Earthquake Engineering* **5**, 149–158. Dynamic interaction between rigid foundations in a layered half-space.
8. Y. Kitamura and S. Sakurai 1979 *Int. J. Analy. Meth. Geomech.* **3**, 159–171. Dynamic stiffness for rectangular rigid foundations on a semi-infinite elastic medium.
9. Y. K. Chow 1986 *Earthquake Engineering & Structural Dynamics* **14**, 643–653. Simplified analysis of dynamic response of rigid foundations with arbitrary geometries.

10. H. TAJIMI 1959 *Rep. Inst. Indust. Sci., University of Tokyo* **8**, 20–30. Basic theories on aseismic design of structures (in Japanese).
11. J. QIAN and D. E. BESKOS 1993 Final Report to the Joint Research Centre of the Commission of the European Communities, Grant No. B/CI1*-923260, Department of Civil Engineering, University of Patras, Patras, Greece. Seismic analysis and design of spread footings.
12. H. L. WONG and J. E. LUCO 1976 *Earthquake Engineering & Structural Dynamics* **4**, 579–587. Dynamic response of rigid foundations of arbitrary shape.
13. M. ABRAMOWITZ and I. A. STEGUN 1972 *Handbook of Mathematic Functions*. New York: Dover.
14. J. E. LUCO and A. MITA 1987 *Earthquake Engineering & Structural Dynamics* **15**, 105–118. Response of a circular foundation on a uniform half-space to elastic waves.
15. F. J. RIZZO, D. J. SHIPPY and M. REZAYAT 1985 Final Project Report for NSF Research Grant CEE-8013461. Boundary integral equation analysis for a class of earth–structure interaction problems.
16. K. YOSHIDA, T. SATO and H. KAWASE 1984 *Proc. Eighth World Conf. on Earthquake Engineering, San Francisco, California*, **III**, 745–752. Dynamic response of rigid foundations subjected to various types of seismic waves.